

## ABSTRACT

Title of Document: THE ISOTOPIC ABUNDANCE OF CESIUM  
IN TRINITITE: IMPLICATIONS FOR POST-  
DETONATION ANALYSIS OF NUCLEAR  
MATERIALS

Dana Tamara Borg, Master of Science, 2013

Directed By: Professor William F. McDonough,  
Department of Geology

Currently, there are few studies of post-detonation materials due to their extremely complex nature. The cesium isotopic composition of trinitite, the product of the first nuclear detonation, was determined using multi-collector inductively coupled plasma mass spectrometry (MC-ICP-MS) to evaluate the relationship between the time since the detonation of nuclear materials and their cumulative fission yields. The ratio of  $^{137}\text{Cs}/^{135}\text{Cs}$  in trinitite was found on average to be  $0.31\pm 0.06$ , with abundances of  $^{137}\text{Cs}$  ( $t_{1/2}=30.07\text{a}$ ) and  $^{135}\text{Cs}$  ( $t_{1/2}=2.3\times 10^6\text{a}$ ) equal to  $21.8\pm 0.6\text{pg/g}$  and  $68\pm 12\text{pg/g}$ , respectively. These values result in an under-calculation of the amount of time that has passed since detonation. It is recommended that an initial  $^{137}\text{Cs}/^{135}\text{Cs}$  ratio of  $1.5\pm 0.3$  be used, instead of the proportion that they are produced during fission of  $^{239}\text{Pu}$   $0.87\pm 0.02$ , due to the fractionation of  $^{137}\text{Cs}$  and  $^{135}\text{Cs}$  before their deposition in trinitite due to the approximately 200 times longer cumulative half-life of the precursors to  $^{135}\text{Cs}$ .

THE ISOTOPIC ABUNDANCE OF CESIUM IN TRINITITE: IMPLICATIONS  
FOR POST-DETONATION ANALYSIS OF NUCLEAR MATERIALS

By

Dana Tamara Borg

Thesis submitted to the Faculty of the Graduate School of the  
University of Maryland, College Park, in partial fulfillment  
of the requirements for the degree of  
Master of Science  
2013

Advisory Committee:  
Professor William F. McDonough, Chair  
Professor Phillip A. Candela  
Professor William B. Walters

© Copyright by  
Dana Tamara Borg  
2013

## Acknowledgements

I would like to thank my thesis advisor, Dr. William F. McDonough, for his continued patience and advice. I would also like to thank my committee members Dr. Philip A. Candela and Dr. William B. Walters for their insight into this project. Much thanks to Dr. Richard Ash for help in the plasma lab, Dr. Philip Piccoli for help with EPMA analyses, Dr. Igor Puchtel for help in the clean lab, and Dr. Katherine Birmingham for helpful discussions and advice. Thanks also to the rest of the McRudnick research group for useful ideas, especially to Nick Sharp, but also including Dr. Roberta Rudnick, Dr. Richard Gaschnig, Dr. Xiaoming Liu, Yu Huang, Kristy Long, Ming Tang, Lauren Stevens, and Su Li. Finally, I would like to thank my fellow graduate students and my family and friends for all of their support and encouragement.

# Table of Contents

Acknowledgements.....	ii
Table of Contents.....	iii
List of Tables.....	iv
List of Figures.....	v
Chapter 1: Introduction.....	1
Trinitite.....	1
Nuclear Forensics and the Comprehensive Nuclear-Test-Ban Treaty.....	3
Fission Product Generation.....	4
Fission Product Distribution.....	7
Chapter 2: Methods.....	10
Samples.....	10
Major Element Analysis.....	11
Sample Preparation.....	12
Chromatography.....	13
Isotopic Analyses.....	14
Evaluation of Time Since Detonation and Cumulative Fission Yields.....	15
Chapter 3: Results.....	17
Major Elements.....	17
Isotopic Analyses.....	18
Time Since Detonation and Fission Yield.....	21
Chapter 4: Discussion.....	24
Bulk Sample Properties.....	24
Isotopic Abundances and Age.....	25
Recommendations for future work.....	29
Chapter 5: Conclusions.....	30
Appendices.....	32
Bibliography.....	35

## List of Tables

Table 1. Measured voltages of Ba in the Ba cuts and reference solutions.....	18
Table 2. Barium isotopic abundances of trinitite compared to natural ratios.....	18
Table 3. Measured voltages in the reference solutions and Cs cuts.....	19
Table 4. Abundances of Ba and Cs recovered from each aliquot of the trinitite sample.....	20

## List of Figures

Figure 1. Arial photo of ground zero 28 hours after the detonation of Trinity.....	2
Figure 2. Comparison of fission yields between $^{239}\text{Pu}$ and $^{235}\text{U}$ fuel sources and the effects on fission yields from high-energy neutrons compared to thermal neutrons in $^{235}\text{U}$ .....	5
Figure 3. Decay chains and half-lives of fission products in the Cs mass.....	6
Figure 4. Reflected light photograph of trinitite samples in an epoxy mount.....	11
Figure 5. Cross section BSE image of trinitite.....	17
Figure 6. $^{137}\text{Cs}/^{135}\text{Cs}$ in trinitite compared to an expected ratio based on their cumulative fission yields.....	20
Figure 7. Relationship between measured $^{137}\text{Cs}/^{135}\text{Cs}$ and time since detonation.....	22
Figure 8. Calculated ages from measured $^{137}\text{Cs}/^{135}\text{Cs}$ .....	23
Figure 9. Initial ratios calculated from actual time since detonation.....	23
Figure 10. Illustration of the fractionation between $^{137}\text{Cs}$ and $^{135}\text{Cs}$ due to the differences in the cumulative half-lives of their precursors.....	27
Figure 11. Relative amount of $^{135}\text{Cs}$ lost based on the calculated initial values of $^{137}\text{Cs}/^{135}\text{Cs}$ .....	27
Figure 12. Comparison of $^{137}\text{Cs}/^{135}\text{Cs}$ values in this study to those from measurements in sediment samples in other studies.....	28

## Chapter 1: Introduction

Fissionogenic cesium isotopes were measured in the post-detonation material trinitite. Analysis of  $^{135}\text{Cs}$  and  $^{137}\text{Cs}$  were completed to investigate the relationship between the fission yield of the isotopes during detonation, fractionation that may occur during the decay chain, and the apparent time that has passed since detonation, based on the time that it takes for these isotopes to decay. This research gives further insights to the practices of post-detonation analyses and implications of their results.

### Trinitite

The nuclear age began on July 16, 1945 with the detonation of the Trinity nuclear test device nicknamed “the gadget” at the Alamogordo Bombing Range, New Mexico. The gadget was a plutonium implosion type device, similar to the bomb that was dropped on Nagasaki, Japan less than a month later. The gadget’s design employed high explosives to compress the spherical core of plutonium, thus increasing its density and driving the core supercritical. At 5:29:45 am, the bomb was detonated atop of a 100 foot steel tower. During the 20 kt-TNT- equivalent detonation (Glasstone and Dolan, 1977) arkosic sand from the desert floor was swept up into the fireball, melted and fell back to the surface, rapidly cooling to form a green glassy layer, 1 to 2 cm thick, becoming the material known as “trinitite” (Figure 1). Trinitite glass is composed of partially melted quartz grains, along with semi-homogenized, melt products of microcline, albite, muscovite, actinolite, and associated gadget-related fragments. X-Ray diffraction shows that the partially melted quartz grains are



the only crystalline phase remaining in trinitite (Eby, 2010). In addition to the green trinitite, “red trinitite” can also be found due to the abundance of Cu in some samples. This variety of trinitite was found to the north of ground zero. As opposed to the majority of trinitite samples that feature the flat-topped morphology of having cooled on the desert floor, also called “pancake trinitite”, there are also trinitite “beads” and “dumbbells”. These are believed to have formed from the molten droplets having cooled in the air before falling to the ground, and are thought to have been transported downwind of the detonation (Eby, 2010).

Included into the glass are fission products, neutron activated products, materials used in the construction of the device, remnants of unfissioned fuel, and naturally occurring radionuclides (Parekh et al. 2006). While this combination adds to the complexity of the material, it potentially also provides useful information about the design of the device, given its chemical and isotopic composition.

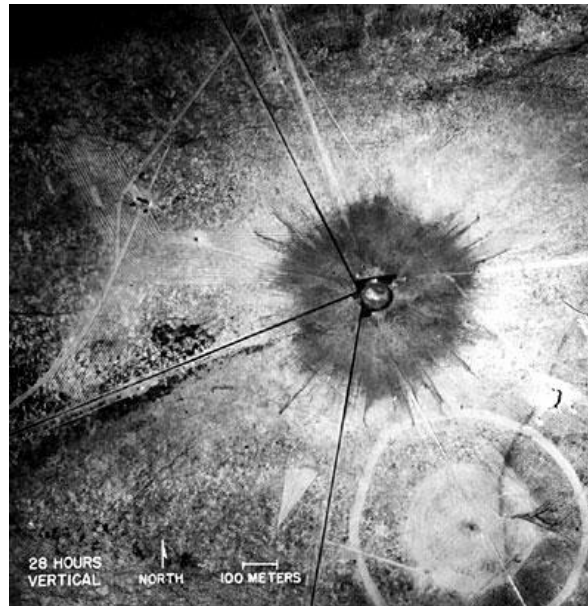


Figure 1. Aerial photo of ground zero 28 hours after the detonation of Trinity. The dark, radiating feature is Trinitite glass. Diameter is ~300m, with spikes increasing the diameter to ~400m. Photo from Los Alamos National Lab.

*Nuclear Forensics and the Comprehensive Nuclear-Test-Ban Treaty*

Nuclear forensics involves the analysis of pre- or post-detonation, nuclear material to enable the identification of a culpable source. In the event of a nuclear detonation, analyses of nuclear debris collected from close proximity to ground zero may reveal isotopic signatures that reflect source and/or yield attributes. Demand for nuclear forensic analyses has grown with the establishment of the US government's Nuclear Forensics and Attribution Act of 2010 that called for the development of protocols to determine the source of both pre- and post-detonation nuclear materials. Currently, there are few post-detonation studies due to the extremely complex nature of the material, thus highlighting the need for such studies.

The Comprehensive Nuclear-Test-Ban Treaty (CTBT, <http://www.ctbto.org/>), which is still not ratified by the United States (05/2013), aims for complete disarmament and ceasing of all nuclear weapons tests and detonations. Participating State Parties agree to not carry out nuclear weapons tests and prohibit such tests from occurring within their jurisdiction. In addition, they agree to refrain from causing or encouraging nuclear detonations by other parties. In order to detect nuclear detonations, the CTBT is establishing the International Monitoring System (IMS, <http://www.ctbto.org/map/#ims>) composing of a system of 170 seismic, 80 radionuclide, 11 hydroacoustic, and 60 infrasound detection stations. Data collected by these stations are processed and analyzed by the International Data Center (IDC).

### Fission Product Generation

In fission events, such as those that occur in nuclear explosions, the fissile material captures a neutron and splits into two separate mass products, one larger and the other smaller, creating a bimodal distribution of isotope species (Figure 2). Energy produced in this reaction comes from the release of the nuclear binding energy; it also releases neutrons that can trigger further fission events, thus creating a chain reaction. The distribution of mass products is a function of the initial fissile material and the energy of the captured neutrons, while the total flux of neutrons controls the amount of the fissile material that undergoes fission, which in turn controls the amount of fission products that are generated. Fast, or high-energy neutrons, as produced in a nuclear explosion, produce a more mono-modal distribution of mass products as compared to thermal (or slow) neutrons. Different fuel sources (e.g.,  $^{235}\text{U}$ ,  $^{239}\text{Pu}$ , etc) also influence mass distribution, where the Trinity test (a  $^{239}\text{Pu}$  device) produced a distinctive mass distribution curve that has a bias to heavier masses compared to other fissile materials (Figure 2).

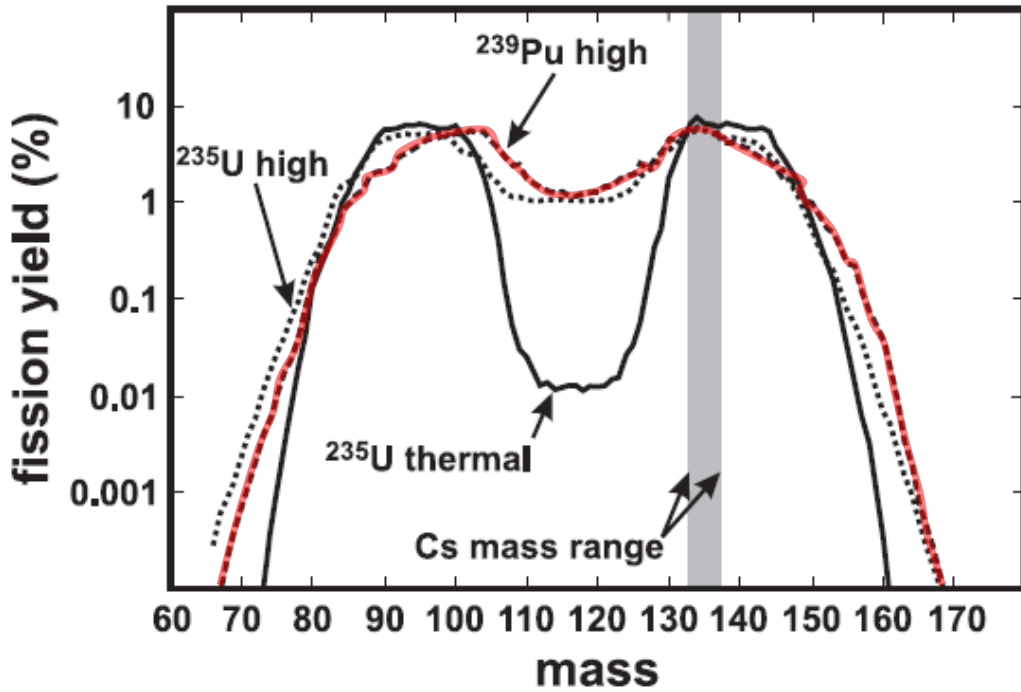


Figure 2. Comparison of fission yields between  $^{239}\text{Pu}$  (red) and  $^{235}\text{U}$  fuel sources and the effects on fission yields from high-energy neutrons compared to thermal neutrons in  $^{235}\text{U}$ . Gray bar illustrates the mass range of Cs isotopes. Figure after Snyder (2012).

The heavier mass peak of the fission yield includes cesium (Cs) isotopes, which are nearly at the top of the peak for both  $^{239}\text{Pu}$  and  $^{235}\text{U}$ . In addition to Cs isotopes produced in the 133 to 137 mass range, isotopes of iodine (I) and xenon (Xe) are produced (Figure 3). These I and Xe isotopes, however, have short half-lives and decay to longer-lived Cs isotopes over seconds to days following the event. After about 20 half-lives, such an isotope can be considered effectively decayed (i.e., below most detection limits). For example, the  $^{137}\text{I}$  ( $t_{1/2} = 24.5$  s) produced in the event will have effectively decayed in less than an hour (i.e.,  $\gg 20$  half-lives), decaying to  $^{137}\text{Xe}$  ( $t_{1/2} = 229$  s), which in turn effectively decays away to  $^{137}\text{Cs}$  in a few hours.

Following that  $^{137}\text{Cs}$  will then decay to  $^{137}\text{Ba}$ , with a 30 year half-life, slow enough to enable this determination (i.e., now only about two half-lives following the event). Cesium-133 is the element's only stable, naturally occurring isotope. Its abundance is enhanced by the addition of fissionogenic  $^{133}\text{Cs}$  and precursor decay products (i.e.,  $^{133}\text{Xe}$  and  $^{133}\text{I}$ ) driving to the valley of nuclear stability, where an isotopic analysis of Xe (stable isotopes at 128-132, 134, and 136) would be useful in determining the amount of  $^{133}\text{Cs}$  that was added to the naturally occurring Cs. These and the other Cs isotopes produced in fission events provide critical evidence of the nature of a nuclear detonation.

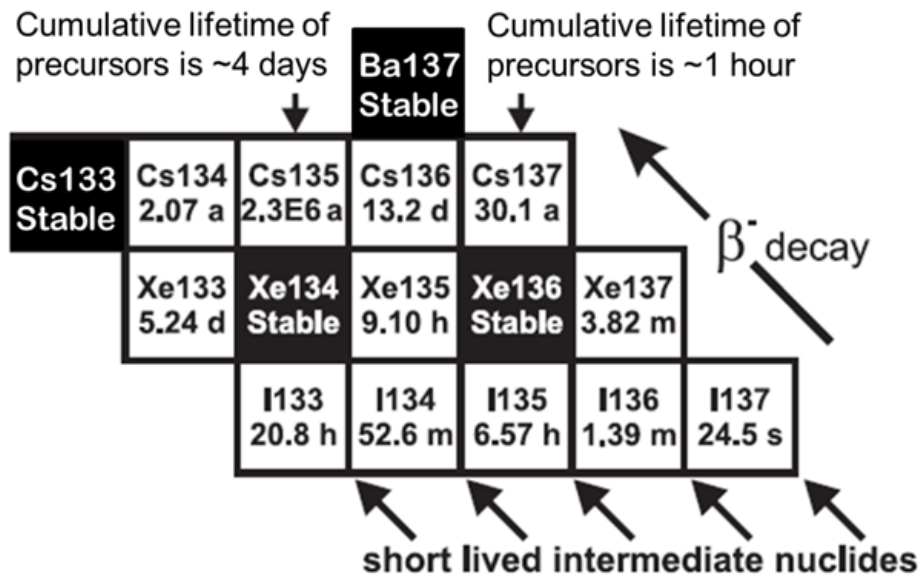


Figure 3. Decay chains and half-lives of fission products in the Cs mass range (133-137amu) Lower mass Cs isotopes are cut off by stable Xe isotopes from 128-132, while higher mass Cs isotopes (i.e. 138-140) decay away in less than a day. Figure after Snyder (2012).

### Fission Product Distribution

Fractionation of fission products can happen and can correlate with distance from ground zero following a nuclear detonation (Snyder, 2012; Belloni, 2011; Lee, 1993). Fractionation results from the varying lengths of the decay chains, or the ‘cumulative half-life’ of the precursors to the isotopes, and separation due to their phase and chemical state (i.e. gas, oxide...). For example, the precursors to  $^{137}\text{Cs}$  are  $^{137}\text{Xe}$  and  $^{137}\text{I}$  (noble and volatile gasses) and their decay to  $^{137}\text{Cs}$  must occur in a closed system within an hour or so in order to avoid phase separation and gross isotopic fractionation. The independent fission yields of  $^{137}\text{Cs}$ ,  $^{137}\text{Xe}$ , and  $^{137}\text{I}$  are 0.7%, 3.7%, and 2.3%, respectively, with  $\beta^-$  half-lives of  $9.48 \times 10^8 \text{ s}$  ( $^{137}\text{Cs}$ ), 229 s ( $^{137}\text{Xe}$ ), and 24.5 s ( $^{137}\text{I}$ ) from  $^{239}\text{Pu}$  (IAEA). Likewise,  $^{135}\text{Cs}$ ,  $^{135}\text{Xe}$  and  $^{135}\text{I}$  have independent fission yields from  $^{239}\text{Pu}$  of 0.006%, 0.8% and 4.3%, with  $\beta^-$  half-lives of  $7.25 \times 10^{13} \text{ s}$  ( $^{135}\text{Cs}$ ),  $3.28 \times 10^4 \text{ s}$  ( $^{135}\text{Xe}$ ), and  $2.37 \times 10^4 \text{ s}$  ( $^{135}\text{I}$ ). Consequently, it takes on the order of 4 days for these precursors to effectively decay to  $^{135}\text{Cs}$ . Thus, the longer-lived beta decay steps to  $^{135}\text{Cs}$  means that its precursors spend a longer time as volatile, mobile species, allowing them to undergo phase separation and be transported further from the detonation site than  $^{137}\text{Cs}$  before decaying and being able to precipitate.

Total system fractionation between  $^{137}\text{Cs}$  and  $^{135}\text{Cs}$  from nuclear detonations has only been assessed in lake sediments at a minimum distance of ~100 miles (~160 km) from the Nevada Nuclear Security Site where numerous nuclear tests were conducted in the 1950's (Snyder, 2012). Reevaluation of the data from Snyder et al (2012) resulted in a  $^{137}\text{Cs}/^{135}\text{Cs}$  ratio at this site to be ~2 once corrected for decay, as compared to the expected  $^{137}\text{Cs}/^{135}\text{Cs}$  ratio of 0.87 based on their fission production

yields. It has yet to be determined if measurable fractionation between  $^{137}\text{Cs}$  and  $^{135}\text{Cs}$  exists on the scale of the radius of the trinitite formation (~300 m).

Belloni et al. (2011) suggested that  $^{152}\text{Eu}$  abundances in trinitite, the activation ( $n,\gamma$ ) product of naturally occurring  $^{151}\text{Eu}$ , varies with distance from ground zero. This relationship was established using gamma-spectroscopy to determine the activity concentrations (Bq/g) coupled with the assumption that there would be a greater neutron fluence nearer to ground zero, thus creating higher concentrations of  $^{152}\text{Eu}$  closer to the point of detonation. Using activities from several trinitite samples, they calculated that each of the samples formed between ~50-70 m from ground zero, with no uncertainties given. However, a comparison of the  $^{152}\text{Eu}$  and  $^{137}\text{Cs}$  activities between the samples shows that there is not a correlation between their concentrations. The lack of correlation suggests that  $^{137}\text{Cs}$  is not evenly distributed between trinitite samples, which is in agreement with Atkaz and Bragg (1995) and Parekh et al. (2006) where  $^{137}\text{Cs}$  activities (normalized to the time of the explosion) are reported to vary over nearly an order of magnitude. It is still unclear whether the lack of correlation between  $^{152}\text{Eu}$  and  $^{137}\text{Cs}$  is a result of fractionation of the fission products within the fireball, or some other process. In addition, it has yet to be determined whether  $^{135}\text{Cs}$  would behave similarly to  $^{137}\text{Cs}$  on the scale of trinitite samples. This could make analysis of the isotopes more difficult in some samples if  $^{135}\text{Cs}$  and  $^{137}\text{Cs}$  behave similarly but are just in lower concentrations. On the other hand, an alternative ratio of the cumulative fission products may have to be used if  $^{135}\text{Cs}$  and  $^{137}\text{Cs}$  are not distributed uniformly on greater than a micron scale.

Few studies on radioactive debris and fallout have included  $^{135}\text{Cs}$ . In addition, ICP-MS measurements of  $^{135}\text{Cs}$  have been difficult as naturally occurring Cs ( $^{133}\text{Cs}$ ) can be up to  $10^9$  times more abundant than  $^{135}\text{Cs}$  (Lee et al., 1993). In addition, both  $^{135}\text{Cs}$  and  $^{137}\text{Cs}$  have direct isobaric interference with natural Ba isotopes with abundances of 6% and 11%, respectively. This interference is enhanced as Ba is ~600 times more concentrated in the upper crust than natural Cs (Rudnick & Gao, 2003).

The fission yields of  $^{137}\text{Cs}$  and  $^{135}\text{Cs}$  and their potential fractionation can be evaluated on the basis of the agreement between the calculated time since detonation ( $t$ ) and the known time that has passed. If there is a fractionation between  $^{137}\text{Cs}$  and  $^{135}\text{Cs}$  on the scale of the detonation site, it results in an underestimation of the amount of time since detonation, reflecting a reduced amount of  $^{135}\text{Cs}$  as it can be dispersed farther than  $^{137}\text{Cs}$  due to the longer amount of time that its parent isotopes spend in noble gas and volatile phases. If this is observed, a fractionation factor can be determined on the basis of distance from ground zero. Understanding any potential fractionation that occurs on this scale will allow for more accurate determination of the time since a nuclear detonation.



## Chapter 2: Methods

### Samples

The trinitite samples in this study are entirely glass with vesicles and contain little to no original desert sand. A typical fragment of trinitite features a green, smooth, flat top which corresponds to the surface during deposition, while deeper into the sample it becomes tan with sandy inclusions (Figure 3). Samples are highly heterogeneous in composition with vesicles accounting for approximately 33% of the total trinitite volume (Hermes and Strickfaden, 2005). The bulk samples are glassy with the exception of some residual quartz grains that remained due to their higher melting point (~1670°C). The proximity of these samples to ground zero at the time of formation is not known.

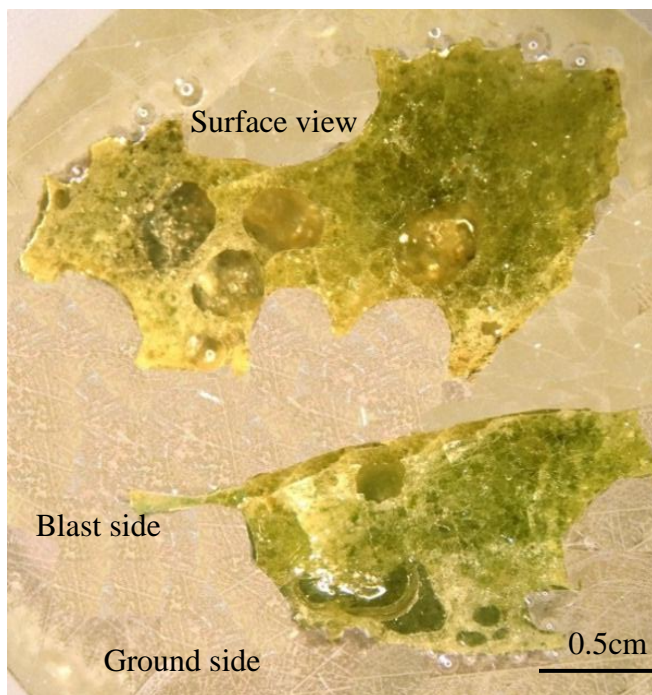


Figure 4. Reflected light photograph of trinitite samples in an epoxy mount, carbon coating removed. Top sample is a surface view; bottom sample is a cross-sectional view featuring a flat top “blast side”, which would correspond to the ground surface when it was deposited. Highly vesicular nature and heterogeneity in glass are visible.

### Major Element Analysis

Major element concentrations were determined by a JEOL JXA-8900 Superprobe electron probe microanalyzer at the University of Maryland, College Park. Analyses were carried out on polished and carbon coated grain mounts (Figure 4) via wavelength dispersive spectrometry (WDS) using an accelerating voltage of 15 kV, a 20  $\mu\text{m}$  spot size, and a 20 nA cup current. Data was recalculated using a ZAF algorithm with kakanui hornblende (Si, Ti, Al, Fe, Mg, Ca, Na), orthoclase (K), and rhodonite (Mn) as primary standards and with Yellowstone rhyolite as a secondary standard.

### Sample Preparation

All labware was cleaned before being introduced to the samples. Savillex screw-top Teflon beakers used in the digestion procedure were cleaned in a process consisting of a 6M Teflon distilled HNO<sub>3</sub> acid flux with ~2mm of acid in the bottom of each sealed beaker and heated at 150°C for 24hr. This process was repeated with Milli-Q H<sub>2</sub>O (i.e., 18MΩ water), then rinsed in Milli-Q H<sub>2</sub>O three times. All pipette tips, centrifuge tubes, and disposable chromatographic columns used throughout the method were cleaned by soaking in 6M Quartz distilled HCl for at least 1 day prior to use, followed by rinsing three times with Milli-Q H<sub>2</sub>O.

For Cs isotopic analysis a two 0.5 g pieces of a single trinitite sample were digested using a standard procedure for rock standards, consisting of a 5:2:0.1 mixture of concentrated HF: HNO<sub>3</sub>: HClO<sub>4</sub> in a sealed 15 mL Teflon beaker. Ultra-pure HNO<sub>3</sub> and HCl (twice quartz distilled, once Teflon distilled) were used in all sample digestions, whereas the HF acid was ultra-pure Seastar acid. The digestion of the sample was performed on a hotplate set to 180°C for a period of 72 hours. After this time, the beaker was opened and the solution allowed to evaporate over the course of a few hours with the temperature gradually increasing from 180°C to 200°C. The residue was then converted to chlorides by adding 1mL of concentrated HCl, resealing and heating at 150°C for an additional 24 hours and drying the sample down again. This process is repeated an additional 2 times. After the 3<sup>rd</sup> drying step, 4 mL of 1.0M Teflon distilled HCl was added to the sample in preparation for chromatography.

### Chromatography

The separation of Cs from its isobaric interference with Ba and the removal of matrix elements were completed using 12cm x 2cm primary columns of Dowex AG50W x8 200-400 mesh cation exchange resin in H<sup>+</sup> form. A 1mL aliquot of the dissolved sample was added to 3 separate columns and washed with an additional 50 mL of the 1.0M Teflon distilled HCl. Next, the Cs cut was collected in the next 20mL of 1.0M Teflon distilled HCl in each of the columns. Five mL of 6.0M Teflon distilled HCl was then added and collected for analysis of the Ba isotopes. The Cs cuts were then dried down and reconstituted in 1mL of 1M Teflon distilled HCl with the process repeated in the primary columns. The Cs cuts were then dried down and dissolved in 0.5mL of 3.0M, Teflon distilled, HNO<sub>3</sub> in preparation for clean-up in a secondary column.

Purification of residual Ba from the Cs cut was done with a 1cm x 0.1cm disposable column with ~0.15mL of Sr-Spec resin. The Cs cuts were loaded into separate Sr-Spec columns and collected in addition to a subsequent 1mL of 3M, Teflon distilled, HNO<sub>3</sub> containing the purified Cs. The Sr-Spec procedure was repeated an additional time for further removal of Ba. The final cuts were dried down and reconstituted in 1mL of 0.8M Teflon distilled HNO<sub>3</sub> for analysis. Total analytical blanks for the complete dissolution and separation procedure were  $0.11 \pm 0.01$  ng ( $1.1 \times 10^{-10}$  kg) for total Ba and  $0.025 \pm 0.002$  ng for <sup>133</sup>Cs.

### Isotopic Analyses

Isotopic analyses of Cs were conducted using the Nu Plasma multi-collector inductively-coupled plasma mass spectrometer (MC-ICP-MS) located in the Plasma Laboratory at the University of Maryland–College Park. Sample analyses were completed using a combination of ion counters and faraday cups with a  $10^{11} \Omega$  resistor array (masses 135 and 137 on ion counters, 138 on faraday cup) and standard bracketing with a 1ppb ( $1 \times 10^{-9}$  kg/kg) pure Ba solution as no radioactive cesium reference material was available. Samples were introduced to the plasma through an Aridus I with a desolvator membrane, using an uptake rate of 50  $\mu\text{L}/\text{min}$ . Analysis time consisted of 100 10-second integrations spaced into five blocks with 30-second,  $\frac{1}{2}$  mass peak background corrections separating each block. Barium isobaric interferences were monitored via  $^{138}\text{Ba}$  during sample acquisition to correct for Ba contamination on  $^{137,135}\text{Cs}$ . During sample acquisition  $^{138}\text{Ba}$  remained stable at  $1.13 \pm 0.01$  mV and required a correction to Cs on masses 137 and 135 using  $^{137}\text{Ba}/^{138}\text{Ba} = 0.1566$  and  $^{135}\text{Ba}/^{138}\text{Ba} = 0.0919$ , each with negligible uncertainties.

Isotope analyses for Ba in Trinitite were conducted on faraday cups alone and were compared to a 50ppb ( $50 \times 10^{-9}$  kg/kg) pure Ba solution. Analysis time consisted of 60 10-second integrations spaced into 3 blocks with 30-second,  $\frac{1}{2}$  mass peak background corrections separating each block. Shorter analysis time was used for the Ba cuts as their signals were on the order of 100 times higher ( $80 \pm 10$  mV) than those measured in the Cs cuts.

### Evaluation of Time Since Detonation and Cumulative Fission Yields

A calculation for the amount of time that has passed since a nuclear detonation, or the age, was made under the assumption that the amount of  $^{137}\text{Cs}$  initially produced is known, using the standard radioactive decay equation (Rutherford and Soddy, 1902):

$$N_t = N_0 e^{-\lambda t}$$

where  $N_t$  is the number of  $^{137}\text{Cs}$  atoms present after a given time;  $N_0$  is the initial number of  $^{137}\text{Cs}$  atoms;  $\lambda$  is the decay constant, which can also be written as  $\frac{\ln 2}{t_{1/2}}$ , where  $t_{1/2}$  is the half-life of  $^{137}\text{Cs}$  and is equal to 30.07a; and  $t$  is time. As there is no direct way of determining the initial amount of  $^{137}\text{Cs}$  produced, a theoretical amount was determined by measuring the amount of  $^{135}\text{Cs}$  in the sample, which has a half-life of  $2.3 \times 10^6$ a, such that even after 100a, only 0.003% of  $^{135}\text{Cs}$  would be lost due to decay. The assumption was therefore made that all of the  $^{135}\text{Cs}$  that was initially produced can be measured today and that there is no fractionation along the decay chain (I to Xe to Cs). From these assumptions, the ratio of the cumulative yields was calculated for a fast neutron flux, ~1MeV, which is the average energy neutron produced in fission events (Byrne, 1996). Given a  $^{239}\text{Pu}$  fuel source of  $^{137}\text{Cs}$  ( $6.35\% \pm 0.12\%$ ) and  $^{135}\text{Cs}$  ( $7.45\% \pm 0.09\%$ ) from the International Atomic Energy Agency (IAEA), yields a relative value of  $^{137}\text{Cs}$  equal to  $0.87 \pm 0.02$  times the amount of  $^{135}\text{Cs}$  (Appendix A). The decay equation can then be written as:

$$^{137}\text{Cs}_t = (0.87 \pm 0.02 \times ^{135}\text{Cs}_t) e^{-\frac{\ln(2)t}{30.07a}}$$

which can be rearranged to solve for  $t$ , where:

$$t = \frac{30.07a}{-\ln(2)} \times \ln\left(\frac{^{137}\text{Cs}_t}{[0.87 \pm 0.02] \times ^{135}\text{Cs}_t}\right)$$

However to test the critical assumption that:

$$^{137}\text{Cs}_0 = (0.87 \pm 0.02) \times ^{135}\text{Cs}_t$$

the Cs isotopes were measured in a post-detonation material where the time of the detonation is known (i.e. trinitite). By knowing how much time has passed since the detonation, the decay of the radioisotopes can be taken into account, which allows for the evaluation of the values of the cumulative fission yields for use when the time since detonation is not known.

## Chapter 3: Results

### Major Elements

Trinitite samples analyzed via an Electron Probe Microanalyzer (EPMA), with a Backscatter Electron (BSE) image revealing a mottled distribution of high- and low-Z domain with a high degree of chemical heterogeneity, as well as the vesicular nature of the samples. Major element concentrations reveal an increase in Fe and Ca with depth, while K and Al decrease with depth (Figure 5 and Appendix B).

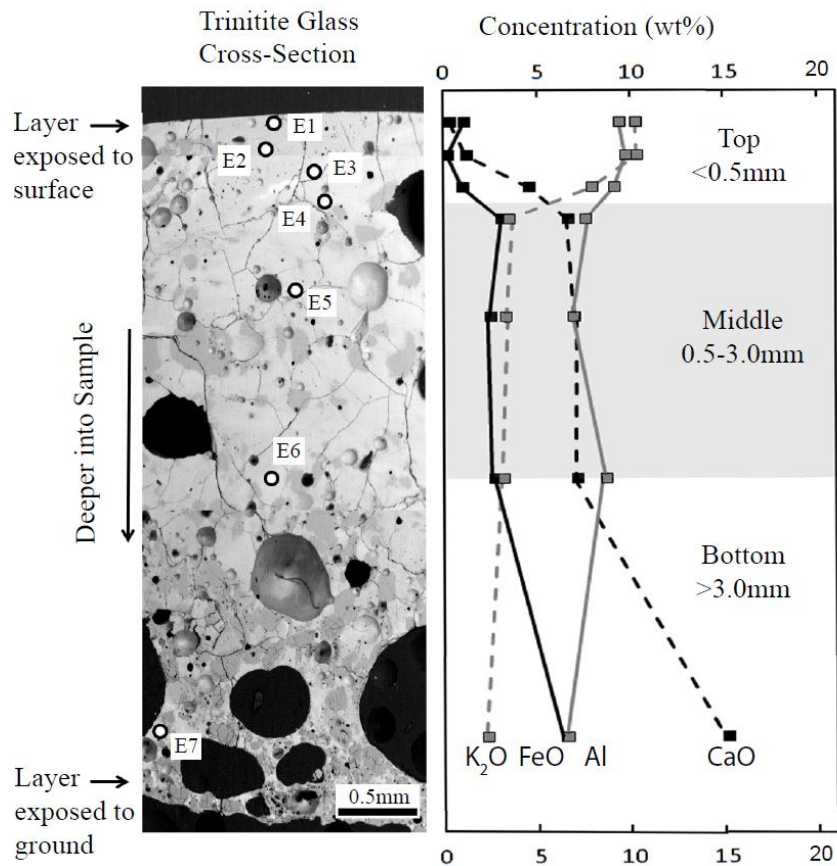


Figure 5: Cross section BSE image of trinitite that shows an increase in size and number of vesicles with depth. Darker shades of gray represent partially melted quartz grains. Uncertainty in the concentration measurements are on the order of  $\pm 1\%$  ( $1\sigma$ ). Data points correspond to those in Appendix B.



Isotopic Analyses

Analysis of isotopic abundances of Ba (138, 137, and 135) in the barium cuts of trinitite agree within  $\pm 2\sigma$  of natural Ba ratios measured in a pure element reference material of Ba (Table 1, 2). Uncertainties on the ratios are on average 5.9% in the reference materials and 4.6% in the samples at the  $\pm 2\sigma$  level. Contributions of fissionogenic Cs are insignificant in the Ba cuts as the measured ratios are not distinguishable from natural.

Sample	138 (V)	$\pm 2\sigma$	137 (V)	$\pm 2\sigma$	135 (V)	$\pm 2\sigma$
50ppb Ba - 1	0.487	0.012	0.075	0.002	0.043	0.001
(TR) Ba - 1	0.086	0.001	0.0132	0.0001	0.0076	0.0001
(TR) Ba - 2	0.101	0.001	0.0155	0.0002	0.0089	0.0001
(TR) Ba - 3	0.062	0.002	0.0096	0.0003	0.0055	0.0001
(TR) Ba - 4	0.115	0.001	0.0178	0.0001	0.0102	0.0001
(TR) Ba - 5	0.102	0.001	0.0158	0.0001	0.0090	0.0001
50ppb Ba - 2	0.218	0.004	0.034	0.001	0.0190	0.0003

Table 1. Measured voltages of Ba (blank subtracted) in the Ba cuts and reference solutions.

Sample	137/135	$\pm 2\sigma$	135/138	$\pm 2\sigma$	137/138	$\pm 2\sigma$
50ppb Ba	1.7	0.1	0.092	0.006	0.16	0.01
(TR) Ba - 1	1.70	0.04	0.092	0.002	0.156	0.004
(TR) Ba - 2	1.70	0.07	0.092	0.004	0.156	0.006
(TR) Ba - 3	1.7	0.1	0.091	0.007	0.16	0.01
(TR) Ba - 4	1.70	0.03	0.092	0.001	0.157	0.002
(TR) Ba - 5	1.71	0.02	0.092	0.001	0.157	0.002
50ppb Ba	1.70	0.08	0.092	0.004	0.157	0.008
Natural Ba	1.7036	-	0.0919	-	0.1566	-

Table 2. Barium isotopic abundances of trinitite samples compared to natural ratios agree within  $\pm 2\sigma$ . Natural ratios from Rosman and Taylor (1997).

Analysis of mass 138 in the Cs cuts of the trinitite samples revealed contaminations on the order of 0.1ppb ( $1 \times 10^{-10}$  kg/kg) Ba remaining corresponding to a signal of  $\sim 1$ mV assuming a  $10^{11}$   $\Omega$  resistor. Subtraction of Ba from masses 137 and 135 are based on natural ratios of  $^{137}\text{Ba}/^{138}\text{Ba}$  and  $^{137}\text{Ba}/^{135}\text{Ba}$  and left approximately  $5\% \pm 2\%$  of the 137 signal and  $15\% \pm 7\%$  of the 135 signal to be Cs (Table 3, 4). The relatively large amount of Ba left in the Cs cut is due to the high blank of the separation process. The Ba subtraction revealed a  $^{137}\text{Cs}/^{135}\text{Cs}$  in trinitite to average  $0.31 \pm 0.06$  with uncertainties of each sample being an average of 24% (Figure 6). The  $^{137}\text{Cs}/^{135}\text{Cs}$  in the trinitite samples is higher than the expected ratio of  $0.18 \pm 0.01$ , which is based upon their cumulative fission yields in a plutonium device.

Sample	138 (V)	$\pm 2\sigma$	137 (V)	$\pm 2\sigma$	135 (V)	$\pm 2\sigma$
1ppb Ba-1	8.22E-03	7E-05	1.23E-03	1E-05	4.94E-04	4E-06
TR-1	9.53E-04	6E-06	1.279E-04	8E-07	5.52E-05	4E-07
TR-2	1.75E-03	1E-05	2.46E-04	2E-06	1.08E-04	1E-06
TR-3	6.90E-04	9E-06	9.9E-05	1E-06	4.58E-05	5E-07
TR-4	7.44E-04	6E-06	1.33E-04	9E-07	5.35E-05	2E-07
TR-5	5.87E-04	6E-06	9.5E-05	3E-06	3.41E-05	1E-06
1ppb Ba-2	1.32E-02	6E-05	1.38E-03	6E-06	4.58E-04	2E-06

Table 3. Measured voltages in the reference solutions and Cs cuts before subtraction of Ba.

Sample	Total Ba	$\pm 2\sigma$	$^{133}\text{Cs}$	$\pm 2\sigma$	$^{137}\text{Cs}$	$\pm 2\sigma$	$^{135}\text{Cs}$	$\pm 2\sigma$
TR-1	380	50	21,000	2,000	22.4	0.5	79	11
TR-2	600	70	170,000	16,000	34.9	0.8	99	18
TR-3	290	30	51,000	5,000	11.7	0.4	36	15
TR-4	300	50	22,000	2,000	23.2	0.6	76	6
TR-5	230	70	16,000	10,000	16.7	0.5	48	11
Average	360	50	56,000	7,000	21.8	0.6	68	12

Table 4. Abundances of Ba and Cs recovered from the Cs cut of each aliquot of the trinitite sample, reported in  $10^{-12}$  kg/kg.

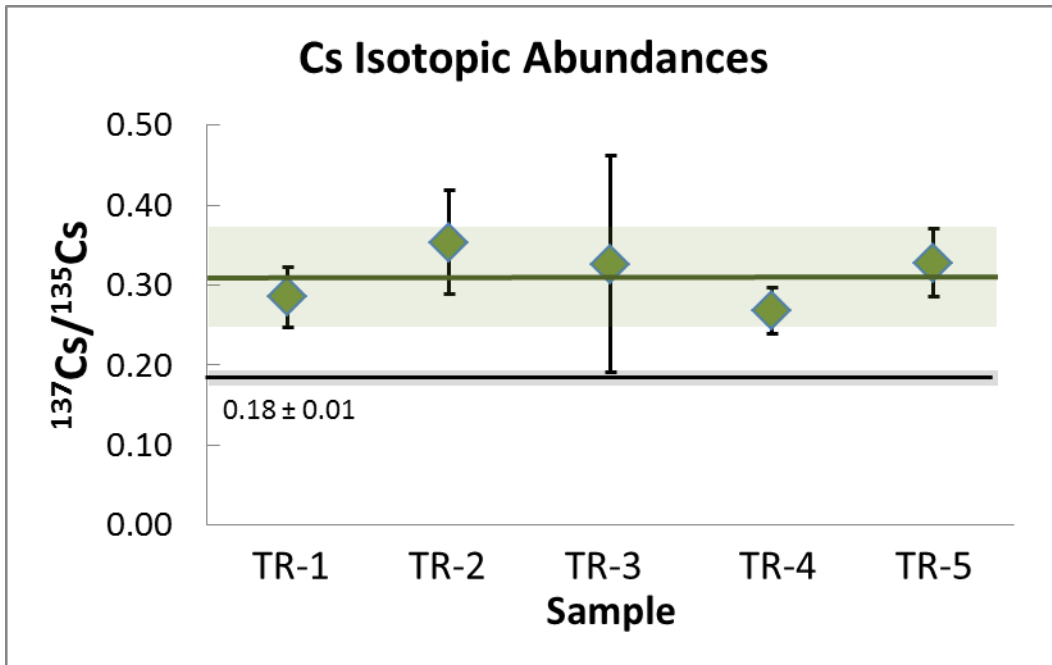


Figure 6.  $^{137}\text{Cs}/^{135}\text{Cs}$  in trinitite compared to an expected ratio ( $0.18 \pm 0.01$ ) based on their cumulative fission yields. Correspond to values in Appendix C.

### *Time Since Detonation and Fission Yield*

Ages were calculated for each sample based on their respective  $^{137}\text{Cs}/^{135}\text{Cs}$ , with an average of  $43_{-8}^{+12}$  years (Figure 7, 8). In addition, all of the calculated ages are less than the actual age of 68 years. These measured  $^{137}\text{Cs}/^{135}\text{Cs}$  were also used to calculate an initial  $^{137}\text{Cs}/^{135}\text{Cs}$  (i.e. the amount recorded in trinitite at the time of detonation) using the actual time that has passed, giving average initial ratios of  $1.5 \pm 0.3$ , which is higher than the expected  $0.87 \pm 0.02$  (Figure 9). Since the age calculations cannot yield symmetrical uncertainties as it is a function of natural logarithms, the uncertainties on the ages and any calculations deriving from them were propagated to determine a maximum and minimum value possible.

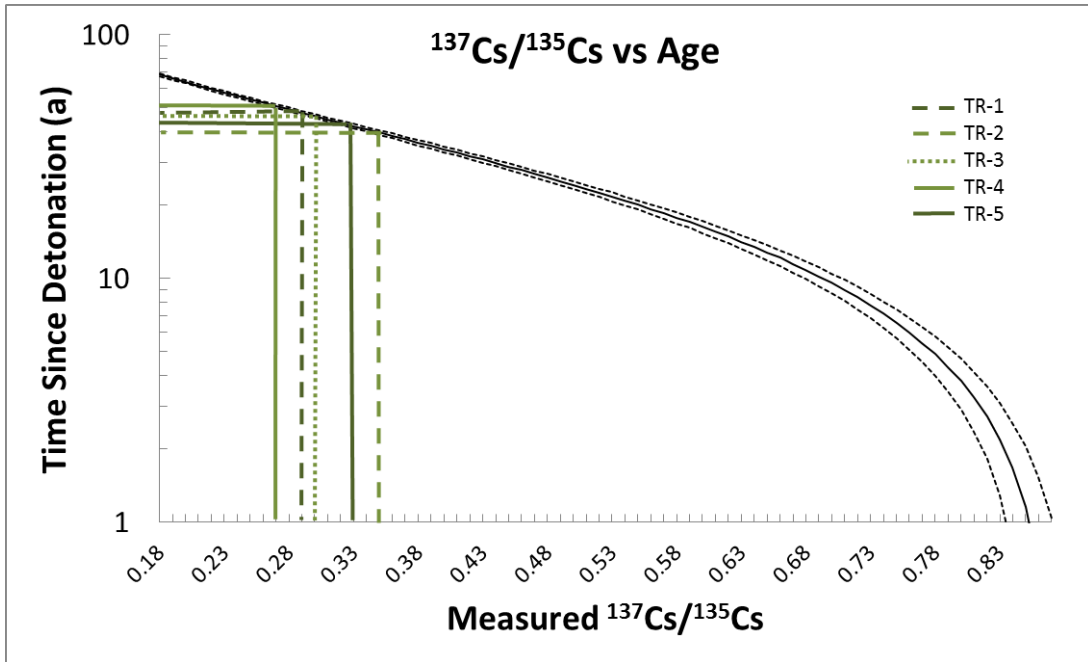


Figure 7. Relationship between measured  $^{137}\text{Cs}/^{135}\text{Cs}$  and time since detonation. Green lines indicate the 5 samples in this study. Solid black line is calculated iteratively based on the decay of  $^{137}\text{Cs}$  assuming an initial  $^{137}\text{Cs}/^{135}\text{Cs} = 0.87$  with intervals of 0.01 to determine the corresponding age for each ratio. Dashed black lines represent the  $\pm 2\sigma$  uncertainty. Uncertainty is not shown for the 3 samples as it is less than the spread in the ratios between the samples. Lines correspond to values in Figures 6 and 8.

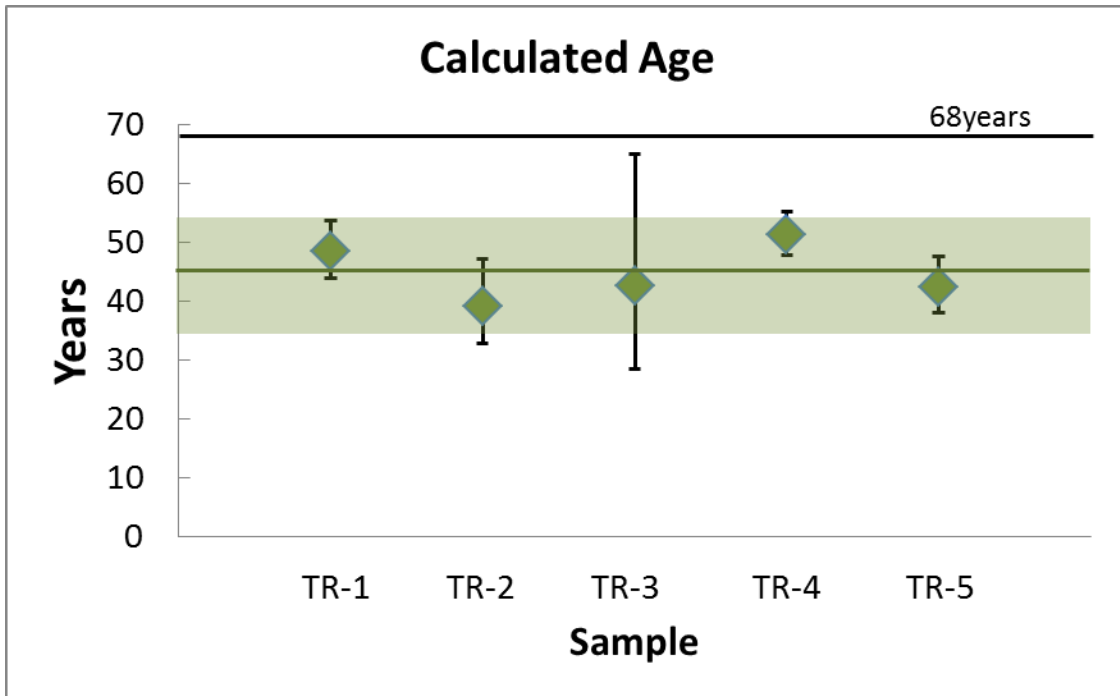


Figure 8. Calculated ages from measured  $^{137}\text{Cs}/^{135}\text{Cs}$ , compared to actual time since detonation of 68 years. Data Points correspond to values in Appendix D.

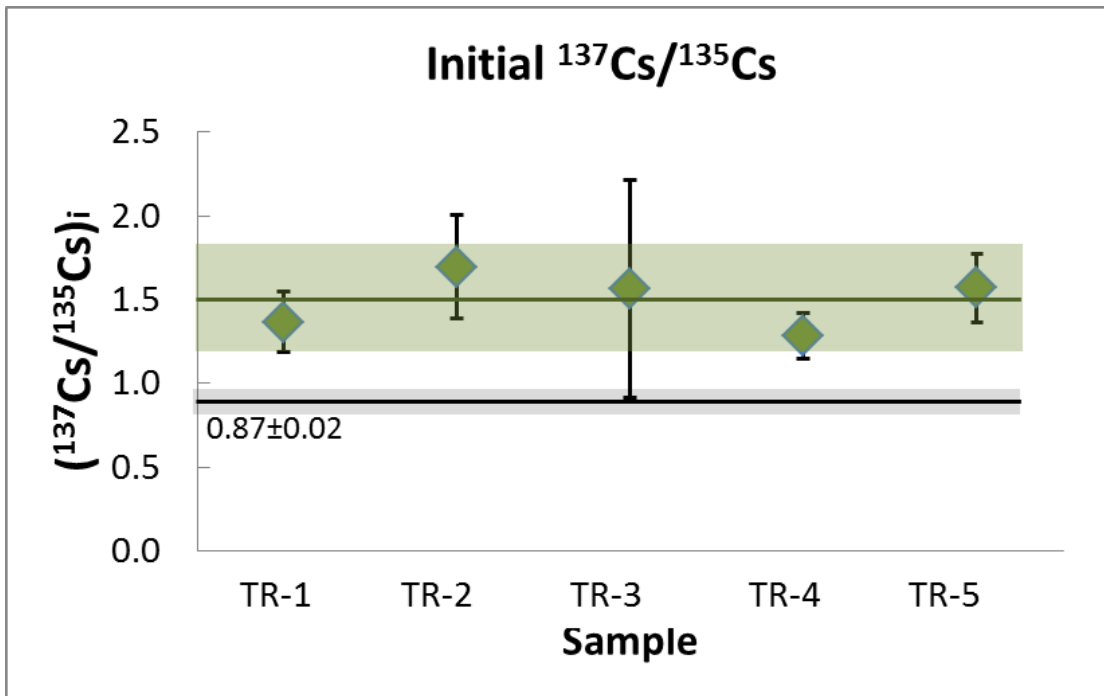


Figure 9. Initial ratios calculated from measured  $^{137}\text{Cs}/^{135}\text{Cs}$  using actual time since detonation (68yrs). Data Points correspond to values in Appendix D.

## Chapter 4: Discussion

### Bulk Sample Properties

Textural and chemical changes with depth from the surface of trinitite samples suggest that the melted material was quenched too rapidly for thermal convection to homogenize the material. The heterogeneity as seen in figure 5 is similar to that seen in previous studies, with compositional variations on the order of 10s of micro meters (Eby, 2010; Fahey, 2010)). The relative enrichment of K and Al, coupled with depletion in Fe and Ca in the top ~1mm of the sample is consistent with observations of a feldspathic glassy matrix on the top of trinitite samples by Ross (1948).

The increase in the size frequency of vesicles with depth in the sample could be due to the degassing of water in the sand underneath the trinitite while it was still molten. The absence of vesicles in the top ~0.1mm of the sample suggests that this could be material that fell from the debris cloud, thus being completely degassed. The subsequent increase in size and number of vesicles suggests that the airborne material could have quickly quenched to act as an insulating layer for the material below. By increasing the cooling time away from the surface, less vapor would have been able to rise to the shallow portions of the sample, compared to the deeper portions, before cooling molten material to the point of vitrification.

### Isotopic Abundances and Age

While theoretically one could use the  $^{137}\text{Cs}/^{135}\text{Cs}$  ratio in a post-detonation material to determine the time that the nuclear bomb was detonated, the results of this study illustrate the need for further study of this isotope system is needed. It is also unlikely that fractionation of the isotopes occurred during the chemical separation process from Ba as no fractionation was observed in the Ba isotopes in the total analytical blank or in the basaltic rock standard BHVO that was analyzed after experiencing the complete dissolution and separation method. Excluding sample heterogeneity and the separation procedure, then that the variability in the  $^{137}\text{Cs}/^{135}\text{Cs}$  is interpreted as a function of the measurement process, not the chromatography procedure. This is supported by the equivalency of the ratios at the  $\pm 2\sigma$  level.

Neutron capture is not expected to have significantly altered the  $^{137}\text{Cs}/^{135}\text{Cs}$  isotopic ratio where  $^{134}\text{Cs}$  and  $^{136}\text{Cs}$  could capture a neutron to become  $^{135}\text{Cs}$  and  $^{137}\text{Cs}$ , respectively, or  $^{135}\text{Cs}$  and  $^{137}\text{Cs}$  could capture a neutron to become  $^{136}\text{Cs}$  and  $^{138}\text{Cs}$ , such that the relative cumulative fission yields of  $^{137}\text{Cs}/^{135}\text{Cs} \neq 0.87$ . This is unlikely to be a factor as the neutron capture cross sections of Cs isotopes 134, 135, 136, and 137 are all approximately 6 barns, for fast neutrons and between 1 and 100 for thermal neutrons (Korea Atomic Energy Research Institute). The cross sections of the precursors to  $^{135}\text{Cs}$  and  $^{137}\text{Cs}$  are all in the same range (5-10b) and are therefore also unlikely to significantly affect the cumulative fission yields by capturing neutrons and disrupting the decay chain.

If neutron capture did not affect the  $^{137}\text{Cs}/^{135}\text{Cs}$  ratio, then the measured ratio should reflect the cumulative fission yields of the isotopes from the detonation of the



nuclear bomb. However, as the measured isotopic ratios and the calculated initial ratios in trinitite are all higher than their expected values, leading to calculated ages that are younger than the actual time since detonation, this study suggests that these isotopes are being fractionated in the time between their production during fission and deposition into trinitite. This phenomenon supports the idea that the difference in the cumulative half-lives of their precursors ( $^{137,135}\text{I}$  and  $^{137,135}\text{Xe}$ ) explains the fractionation of  $^{137}\text{Cs}$  and  $^{135}\text{Cs}$ .

Due to the volatility of iodine, with a boiling point of  $184^\circ\text{C}$ , it would be unable to condense and precipitate, thus inhibiting its incorporation into trinitite. As the decay product of fissionogenic iodine, xenon, would also remain as a gas before decaying to cesium, it is unlikely to be included as well. As both I and Xe would remain airborne, they can be dispersed away from the detonation site with blowing wind.

Since the gaseous precursors to  $^{135}\text{Cs}$  ( $^{135}\text{I}$  and  $^{135}\text{Xe}$ ) have much longer half-lives than those of  $^{137}\text{Cs}$ , cumulatively  $\sim 200$  times longer, it is possible that a relatively larger amount of  $^{135}\text{Cs}$  can be transported away from the detonation site before decaying to Cs, at which point it would bind with another ion to become a solid and precipitate from the debris cloud (Figure 10). The relative amount of  $^{135}\text{Cs}$  that was lost compared to  $^{137}\text{Cs}$  was calculated from the values of the initial  $^{137}\text{Cs}/^{135}\text{Cs}$ . In order to have the initial ratios recorded in trinitite (average  $1.5 \pm 0.3$ ) an average of  $43_{-8}^{+12}\%$  of the  $^{135}\text{Cs}$  would have been lost, assuming that at the time of production  $^{137}\text{Cs}/^{135}\text{Cs}$  was  $0.87 \pm 0.02$  (Figure 11).

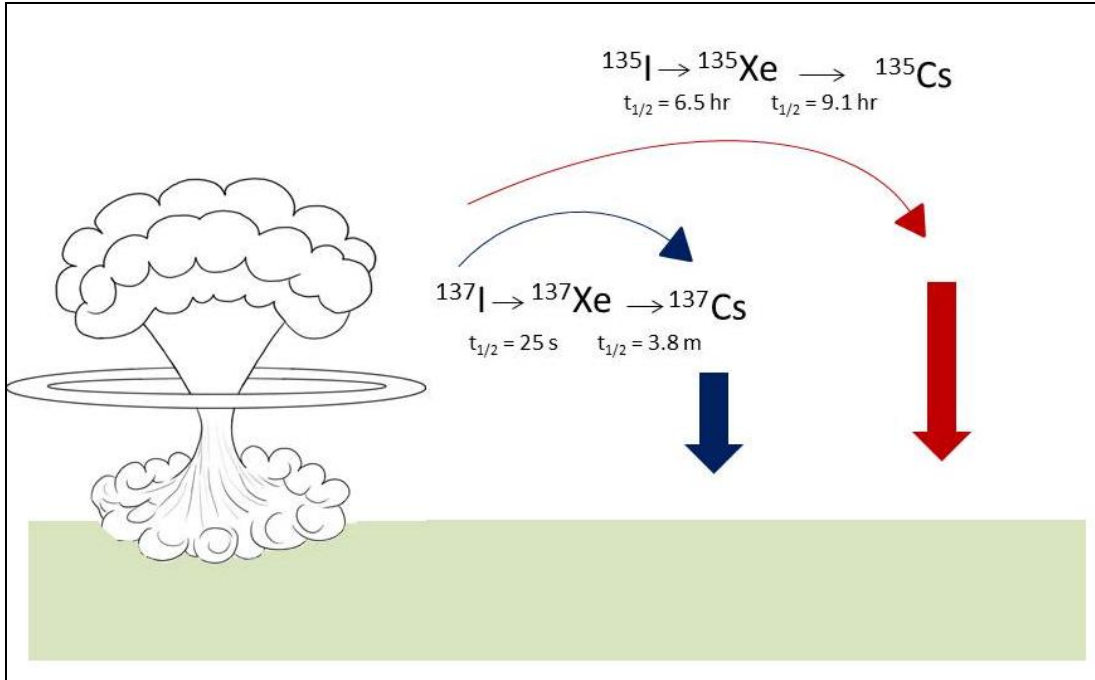


Figure 10. Illustration of the fractionation between  $^{137}\text{Cs}$  and  $^{135}\text{Cs}$  due to the differences in the cumulative half-lives of their precursors where I and Xe would remain gases before decaying to Cs and becoming a solid.

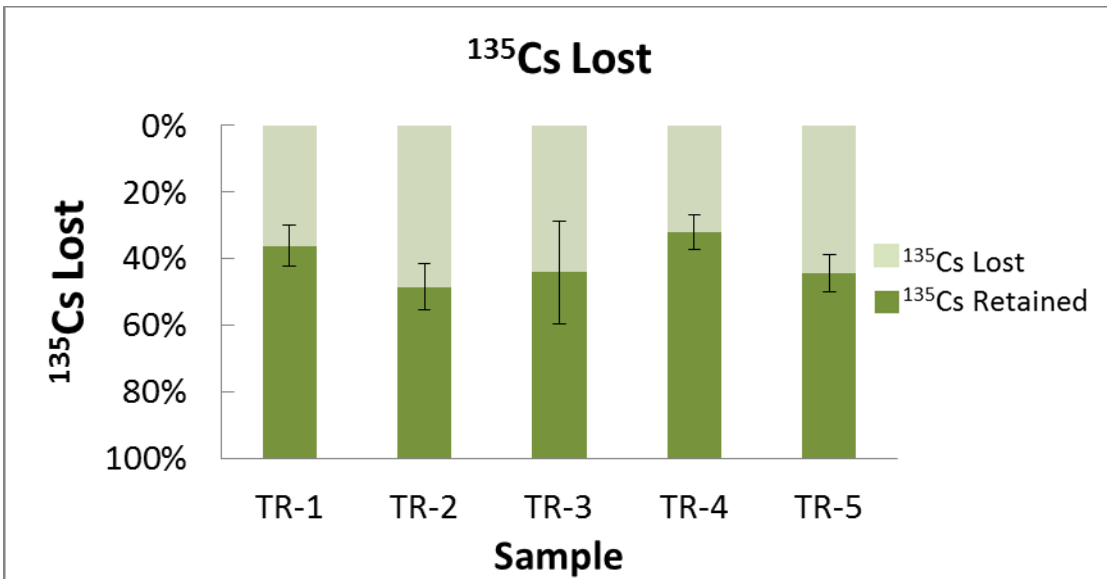


Figure 11. Relative amount of  $^{135}\text{Cs}$  lost based on the calculated initial values of  $^{137}\text{Cs}/^{135}\text{Cs}$ . Correspond to values in Appendix E.

A comparison of the  $^{137}\text{Cs}/^{135}\text{Cs}$  measured in trinitite in this study to those reported in two other studies that have measured both  $^{137}\text{Cs}$  and  $^{135}\text{Cs}$  in sediment samples to date shows that the ratios are significantly lower in this study (Figure 12). However, the samples in the other studies were taken at a much greater distance from a nuclear detonation than the trinitite from this study (Lee: San Francisco Bay; Snyder: Sandhole Lake, Idaho and Lake Meade, Nevada). It is likely that as these sites are farther away from a detonation site, the fractionation would be more pronounced, thus creating higher  $^{137}\text{Cs}/^{135}\text{Cs}$  ratios. In addition, these values would not reflect the cesium isotopic abundances of a single detonation, but more likely the signatures of many detonations of both plutonium and uranium devices. As measurements of  $^{135}\text{Cs}$  are so few, these are unfortunately the only comparisons of  $^{137}\text{Cs}$  and  $^{135}\text{Cs}$  deposition that can be made.

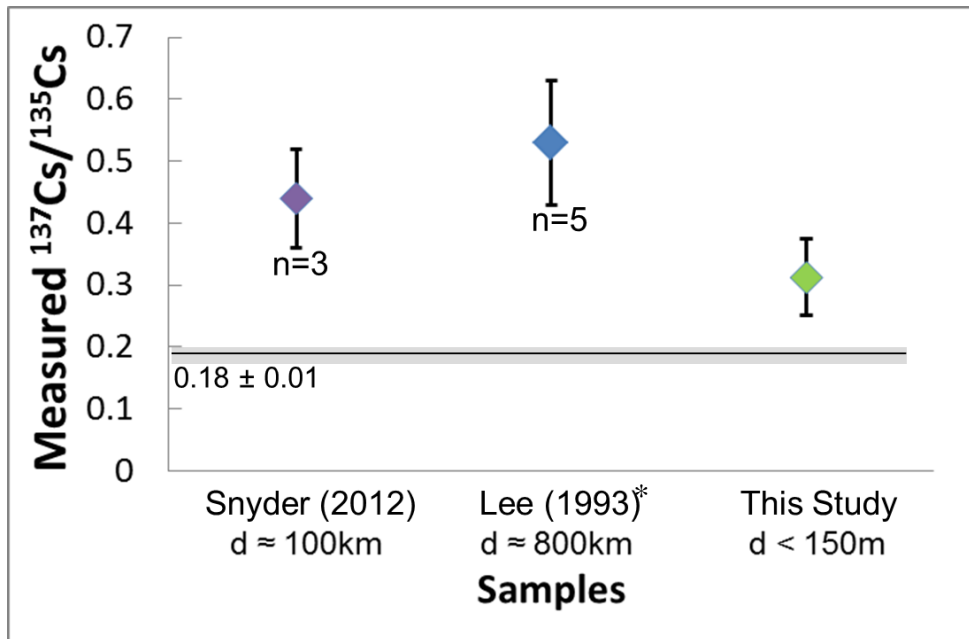


Figure 12. Comparison of  $^{137}\text{Cs}/^{135}\text{Cs}$  values in this study to those from measurements from sediment samples in other studies. \*Re-calculated to 2013.

In all cases, an initial  $^{137}\text{Cs}/^{135}\text{Cs} = 0.87$  would be inappropriate to apply to samples for the purpose of calculating a time since detonation. However, as the sample in this study was the closest to a nuclear detonation, they would be more suitable for determining a reliable initial  $^{137}\text{Cs}/^{135}\text{Cs}$  value for post-detonation nuclear materials. With the measurements in trinitite to date, the best suggestion that would be made is for an initial values of  $^{137}\text{Cs}/^{135}\text{Cs} = 1.5 \pm 0.3$ .

#### Recommendations for future work

In order to constrain better the initial values of  $^{137}\text{Cs}/^{135}\text{Cs}$  for the use in dating nuclear detonations, further study is needed. Analysis of  $^{137}\text{Cs}/^{135}\text{Cs}$  in multiple pieces of trinitite should be made to determine the variability in the distribution of these isotopes. As the exact location of the sample that was used in this study in relation to ground zero of the detonation is unknown and only one single piece of trinitite was analyzed, the relationship between  $^{137}\text{Cs}/^{135}\text{Cs}$  and the distance from detonation cannot be precisely determined.

In addition, samples should be analyzed from a uranium detonation (i.e. Hiroshima), as trinitite was produced from a plutonium device. As  $^{137}\text{Cs}$  is produced at a slightly higher rate than  $^{135}\text{Cs}$  in the fission of  $^{235}\text{U}$  ( $^{137}\text{Cs}/^{135}\text{Cs} = 0.93$ ), a separate initial value of  $^{137}\text{Cs}/^{135}\text{Cs}$  may be needed to calculate the age of a uranium detonation.

## Chapter 5: Conclusions

The observations of trinitite samples in this study are comparable to those made in previous studies. The relative enrichment of K and Al at the surface of trinitite is likely the remnants of melted potassium feldspar grains that did not completely diffuse into the surrounding glass. The highly vesicular nature of the samples is believed to be due to the degassing of water from the underlying sand. The vesicles deeper in the sample are larger as the material there stayed molten longer as it was insulated by the quenched glass at the surface.

The measured  $^{137}\text{Cs}/^{135}\text{Cs}$  in the dissolved trinitite sample averages  $0.31 \pm 0.06$  which is higher than the expected ratio from the fission of  $^{239}\text{Pu}$  68 years ago. It is suggested that this higher result is due to fractionation during the time that the precursors of  $^{137}\text{Cs}$  and  $^{135}\text{Cs}$  remain as gasses, allowing relatively more  $^{135}\text{Cs}$  isobars to travel away from the detonation site before precipitating. The higher  $^{137}\text{Cs}/^{135}\text{Cs}$  that was measured would lead to the under-calculation of the amount of time that has passed since detonation if it is assumed that both isotopes were incorporated into trinitite in the ratio based solely on their cumulative fission yields of  $^{137}\text{Cs}/^{135}\text{Cs} = 0.87 \pm 0.02$ . It is recommended that due to the fractionation of the isotopes before their deposition in trinitite, an initial  $^{137}\text{Cs}/^{135}\text{Cs} = 1.5 \pm 0.3$  be used for calculations of the amount of time that has passed since detonation.

More work is needed to better constrain the initial  $^{137}\text{Cs}/^{135}\text{Cs}$  for use in age calculations for  $^{239}\text{Pu}$  devices as it has yet to be determined how these isotopes vary

in trinitite. The debris from a  $^{235}\text{U}$  device should also be analyzed in order to determine if a separate value for the initial  $^{137}\text{Cs}/^{135}\text{Cs}$  should be used in calculating the amount of time that has passed since the detonation of a U bomb.

## Appendices

### Appendix A

	137	t <sub>1/2</sub>	135	t <sub>1/2</sub>
Sn	0.000001%	190ms	0.002%	530ms
Sb	0.004%	492ms	0.9%	1.7s
Te	2%	2.49s	30%	19.0s
I	34%	24.5s	58%	6.58h
Xe	55%	3.8m	11%	9.14h
Cs	9%	30.07a	0.1%	2.3E6a

Appendix A: Relative proportions of each isotope produced at masses 137 and 135 during the fission of <sup>239</sup>Pu, contributing to the cumulative fission yields of <sup>137</sup>Cs and <sup>135</sup>Cs, and their half-lives (Brookhaven National Lab).

### Appendix B

	E1	E2	E3	E4	E5	E6	E7
<i>Oxide wt%</i>							
SiO <sub>2</sub>	64.74	64.96	65.43	67.72	68.14	65.52	57.10
TiO <sub>2</sub>	0.08	0.03	0.08	0.54	0.45	0.37	0.92
Al <sub>2</sub> O <sub>3</sub>	18.81	19.46	18.21	15.25	13.86	17.31	13.25
FeO	1.15	0.28	1.05	3.15	2.53	2.71	6.57
MnO	0.02	0.00	0.02	0.07	0.06	0.06	0.09
MgO	0.39	0.03	0.44	1.30	1.06	1.00	2.74
CaO	0.38	1.27	4.62	6.66	7.00	7.10	15.15
Na <sub>2</sub> O	2.14	2.61	2.05	2.09	1.82	2.21	1.71
K <sub>2</sub> O	10.25	10.32	7.92	3.55	3.32	3.17	2.32
Total	97.96	98.96	99.82	100.33	98.24	99.45	99.85

Appendix B: Major element oxide composition obtained via EPMA analysis of trinitite. Sample site labels correspond to locations in Figure 5.

Appendix C

Sample	$^{137}\text{Cs}/^{135}\text{Cs}$	$\pm 2\sigma$	RSD%
TR-1	0.29	0.04	13%
TR-2	0.35	0.06	18%
TR-3	0.3	0.1	42%
TR-4	0.27	0.03	11%
TR-5	0.33	0.04	13%
Average	0.31	0.06	20%
Expected Today	0.18	0.01	-
Initial Expected	0.87	0.02	-

Appendix C:  $^{137}\text{Cs}/^{135}\text{Cs}$  in trinitite compared to an expected ratio based on their cumulative fission yields. Values correspond to those in Figure 6.

Appendix D

Sample	Calculated Age (yr)	Initial $^{137}\text{Cs}/^{135}\text{Cs}$
TR-1	$49^{+5}_{-5}$	$1.4\pm 0.2$
TR-2	$39^{+8}_{-6}$	$1.7\pm 0.3$
TR-3	$43^{+22}_{-14}$	$1.6\pm 0.7$
TR-4	$51^{+4}_{-3}$	$1.3\pm 0.1$
TR-5	$42^{+5}_{-4}$	$1.6\pm 0.2$
Average	$45^{+9}_{-7}$	$1.5\pm 0.3$
Expected	68	$0.87\pm 0.02$

Appendix D. Calculated ages from measured  $^{137}\text{Cs}/^{135}\text{Cs}$ . Initial ratios calculated from actual time since detonation. Values correspond to those in Figures 7 and 8.



Appendix E

Sample	$^{135}\text{Cs}$ Lost
TR-1	$36^{+6}_{-8}\%$
TR-2	$48^{+7}_{-10}\%$
TR-3	$44^{+16}_{-38}\%$
TR-4	$32^{+5}_{-6}\%$
TR-5	$44^{+5}_{-7}\%$
Average	$41^{+8}_{-14}\%$

Appendix E. Relative amount of  $^{135}\text{Cs}$  lost based on the calculated initial values of  $^{137}\text{Cs}/^{135}\text{Cs}$ . Values correspond to those in Figure 11.

## Bibliography

- Atkatz, D., and C. Bragg, 1995, Determining the yield of the Trinity nuclear device via gamma-ray spectroscopy: *American Journal of Physics*, v. 63, p. 411-413.
- Belloni, F., J. Himbert, O. Marzocchi, and V. Romanello, 2011, Investigating incorporation and distribution of radionuclides in trinitite: *Journal of Environmental Radioactivity*, v. 102, p. 852-862.
- Byrne, J. 1996. *Neutrons, Nuclei, and Matter*, Dover Publications, Mineola, NY, 2011, ISBN-13 978-0-486-48238-5
- Eby, N., Hermes, R., Charnley, N., and Smoliga, J. A., 2010, Trinitite-the atomic rock, *Geology Today*, Volume 26.
- Fahey, A. J., Zeissler, C. J., Newbury, D. E., Davis, J., and Lindstrom, R. M., 2010, Postdetonation nuclear debris for attribution: *Proceedings of the National Academy of Sciences of the United States of America*, v. 107, no. 47, p. 20207-20212.
- Glasstone, S., and P. J. Dolan, 1977, *The Effects of Nuclear Weapons*, Third Edition, Washington: U.S. Government Printing Office.
- Hermes, R., and W. Strickfaden, 2005, A new look at trinitite, *Nuclear Weapons Journal*, p. 2-7.
- Lee, T., T.-L. Ku, H.-L. Lu, and J.-C. Chen, 1993, First detection of fallout Cs-135 and potential applications of  $^{137}\text{Cs}/^{135}\text{Cs}$  ratios, *Geochimica et Cosmochimica Acta*, p. 3493-3497.
- Parekh, P. P., T. M. Semkow, M. A. Torres, D. K. Haines, J. M. Cooper, P. M. Rosenberg, and M. E. Kitto, 2006, Radioactivity in Trinitite six decades later: *Journal of Environmental Radioactivity*, v. 85, p. 103-120.
- Rosman, KJR., Taylor, PDP., 1997, *Isotopic Compositions of the Elements 1997*. International Union of Pure and Applied Chemistry.
- Ross, CS (1948) *Optical Properties of Glass from Alamogordo, New Mexico*. *American Mineralogist*, Vol: 33.
- Rudnick, R., and S. Gao, 2003, *Composition of the Continental Crust-3.01*.

Rutherford, E., and F. Soddy, 1902, XLI. The cause and nature of radioactivity.—  
Part I, Philosophical Magazine Series 6. 4 (21), p. 370-396.

Snyder *et al.*, 2012, Radioactive cesium isotope ratios as a tool for determining  
dispersal and re-dispersal mechanisms downwind from the Nevada  
Nuclear Security Site, Journal of Environmental Radioactivity, p. 46-52.